Dispersion Relations for Phonons in Aluminum at 80 and 300°K

R. STEDMAN AND G. NILSSON
AB Atomenergi, Studsvik, Sweden
(Received 29 November 1965)

The dispersion relations for aluminum have been determined at 80 and 300°K by neutron spectrometry, using a three-axis crystal spectrometer. Particular attention was paid to precision, in order to investigate small effects—e.g., Kohn anomalies, phonon frequency widths, frequency shifts with temperature—and to establish an accurate experimental routine. A focusing method used throughout to optimize resolution is described, as well as a method for calculating energy resolution and extracting phonon widths from observed one-phonon resonances. Results are presented as dispersion curves for phonons in the three principal directions, accompanied by phonon widths, and as contour maps of phonon frequency on the surface of an elemental tetrahedron in **q** space. Measurements at points off the principal directions are utilized in the latter maps. Kohn anomalies have been observed, but are reported elsewhere. Phonon widths at 80°K are interpreted semiquantitatively in terms of the interaction between phonons and conduction electrons. Exceptionally large phonon widths in two regions may be due to singularities in the phonon-phonon interaction: the conservation rules for decay of a phonon into two phonons suggest a source for such singularities, but the suggestion has not been confirmed by computation.

1. INTRODUCTION

THE dispersion relations for phonons in aluminum have been determined at 80 and 300°K by neutron spectrometry, using a three-axis crystal spectrometer operating at Studsvik's 30-MW research reactor R2. The results include frequencies for phonons with wave vectors in the three principal directions, and for sufficient wave vectors in other directions to permit good interpolation of frequencies over a cell of the wave-vector space. In addition, frequency widths of phonons have been derived from most of the observed one-phonon resonances. Results are presented as dispersion curves for the three principal directions, accompanied by corresponding phonon widths, and as contour maps of phonon frequency.

The dispersion curve for longitudinal phonons in the [2,2,0] direction was determined in particular detail, partly because this happened to be the dispersion curve we first dealt with and we made many repeated or similar measurements to test experimental improvements, and partly because we became engaged in a search for Kohn anomalies. These latter small irregularities eluded us at the time, and on subsequent dispersion curves we were content to make less detailed measurements. Lately, however, improved analysis of data and supplementary measurements have revealed Kohn anomalies in several places; the results have been published elsewhere,[1] and will not be considered here.

During the course of our measurements, we became aware that certain disturbances are more troublesome than might be supposed at first sight. They are peaks associated with such things as second-order reflection in the analyzer crystal, or Bragg scattering in the sample. Such a peak, if small and undetected, may give rise to a spurious shift and broadening of a one-phonon resonance. We took pains to eliminate effects of this sort. They are treated very briefly here, as are also some other aspects of the experimental method—focusing (a technique used throughout to optimize resolution), resolution, and errors.

[1] R. Stedman and G. Nilsson Phys. Rev. Letters **15**, 634 (1965).

2. THE SPECTROMETER AND ITS MODE OF OPERATION

A full description of the spectrometer will be published shortly. It is of course similar in principle to other three-axis spectrometers—a monochromator crystal in a beam from the reactor directs a beam of monoenergetic neutrons at the sample crystal,[2] and from there neutrons scattered in a particular direction enter the analyzer, which can count only those with a given energy.

The important variables are the change of neutron momentum on scattering ($\mathbf{K}$) and the change of energy (ϵ). At any setting of the spectrometer, the mean values of these variables are known, and we may say that the spectrometer looks at the sample's scattering cross section at a point $(\mathbf{K},\epsilon)$ [3] (actually, of course, a small region around this point, but for the moment resolution considerations may be neglected). This point moves as the spectrometer setting is changed, and when it passes through a surface on which one-phonon resonances occur in the scattering cross section, the spectrometer records a peak. The resonance surface is a direct image of the dispersion surface for phonons, $\omega=\omega(\mathbf{Q})$, through the resonance condition, $(\mathbf{K},\epsilon)=(\mathbf{Q},\omega)$[4]. The condition

[2] In the present case an aluminum crystal with narrow mosaic width (the rocking curve was 0.15° wide at half-maximum), kindly lent by D. H. Saunderson of Harwell, and made by Metals Research Ltd., Cambridge, England.

[3] The cross section depends on k_1 and the sample geometry, as well as on $(\mathbf{K},\epsilon)$, but the variation of these factors within the small range of spectrometer movements required for a measurement on on a one-phonon resonance is negligible.

[4] The units are such that $\hbar$ and the neutron mass are both unity. $\mathbf{K}=\mathbf{k}_1-\mathbf{k}_2$, $\epsilon=\frac{1}{2}(k_1^2-k_2^2)$, where $\mathbf{k}_1$ is the wave vector of a neutron before scattering and $\mathbf{k}_2$ is the wave vector after scattering. ω is the frequency of a phonon, $\mathbf{Q}$ is its wave vector referred to the origin, corresponding to the reduced form $\mathbf{q}$ when referred to the reciprocal lattice point $\mathbf{G}$ which is in the same cell of reciprocal space ($\mathbf{Q}=\mathbf{q}+\mathbf{G}$).

corresponds to excitation of a single phonon by a neutron when ϵ and ω are positive.

In the present measurements $\mathbf{K}$ was kept constant (with respect to the sample), and ϵ varied in equal steps. Spectrometer movements are in multiples of 0.01°, and follow a program tape. The constant-$\mathbf{K}$ program involves coordinated small changes of the monochromator angle, sample orientation, and scattering angle. The analyzer setting remains constant, so the sensitivity of the analyzer does not change during a measurement. Counting periods are determined by a monitor in the beam entering the sample, which means that the intensity variations at the monochromator are also without significance.

The collimators immediately before and after the sample are readily exchangeable, collimation angles being chosen as small as the intensity available in a given measurement allows in order to reduce the uncertainty in momentum transfer to a minimum. Energy resolution also improves when collimation angles are reduced, but can be improved without the reduction of intensity that finer collimators entail by applying a focusing technique (described briefly in Sec. 3).

Available intensity must of course be assessed in relation to the background. Our background has been pared down to 15–20 counts per hour (disregarding thermal neutrons from the sample) by careful attention to shielding and the use of a quartz filter in the beam from the reactor. The filter is similar in dimensions and performance to one described by Brockhouse[5]; it removes fast neutrons (attenuation factor 40) and resonance neutrons (attenuation factor 100) from the beam much more than it does thermal neutrons (average attenuation 3).

3. FOCUSING

The idea of focusing may be visualized by regarding the shape of the region around the point $(\mathbf{K},\epsilon)$ seen by the spectrometer (mentioned in Sec. 2). The shape is that of an intensity distribution with its mean and maximum at $(\mathbf{K},\epsilon)$. If the plane of scattering is horizontal, small vertical increments to $\mathbf{k}_1$ and $\mathbf{k}_2$ (mean values for the neutrons from the monochromator and those accepted by the analyzer) do not affect ϵ, nor do the corresponding increments applied to $\mathbf{Q}$ affect $\omega(\mathbf{Q})$ if the sample exhibits reflection symmetry with respect to the plane of scattering (the usual case); consequently we may neglect the vertical dimension of $\mathbf{K}$ in considering energy resolution, and use a picture with two dimensions of $\mathbf{K}$ horizontal and ϵ vertical. Figure 1 is a sectional illustration of the intensity distribution around $(\mathbf{K},\epsilon)$, the surface of one-phonon resonances (dispersion surface), and the resonance peak recorded as the spectrometer moves. Intensity distributions are represented by half-maximum contours, that for the distribution around $(\mathbf{K},\epsilon)$ being to a good approximation an ellipsoid, which retains the same shape and

[5] B. N. Brockhouse, Rev. Sci. Instr. **30**, 136 (1959).

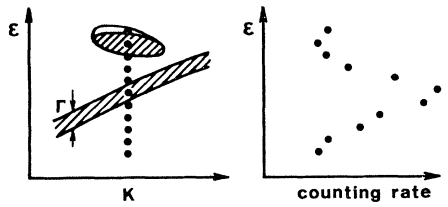

FIG. 1. The correspondence between the spectrometer's traversing of a dispersion surface (left) and a one-phonon resonance (right). Widths of distributions are indicated by half-maximum contours, shown in section.

orientation during the small spectrometer movements involved in recording a one-phonon resonance. The ellipsoid is thin (its diameter in the ϵ direction is small compared to the over-all ϵ dimension), and it is possible to arrange an experiment so that this thin disk is approximately parallel to the dispersion surface at the point under investigation, whereby the observed resonance becomes narrower and higher than it would otherwise have been. The method is called focusing.

A closer examination of focusing requires an analysis of the intensity distribution around $(\mathbf{K},\epsilon)$ in terms of experimental parameters. Suppose first that the incident and scattered beams are very finely collimated, and the mosaic widths of monochromator and analyzer are small; then $\mathbf{k}_1$ and $\mathbf{k}_2$ are narrowly determined, and we may regard the distribution as localized to $(\mathbf{K},\epsilon)$. If the entrance collimator is now widened, the distribution becomes linear in the direction $(\Delta_c\mathbf{k}_1,\ \mathbf{k}_1\cdot\Delta_c\mathbf{k}_1)$, where $\Delta_c\mathbf{k}_1$ is the width of the distribution of incident neutron momenta about the mean $\mathbf{k}_1$ corresponding to the now appreciable collimation angle ($\Delta_c\mathbf{k}_1$ is parallel to the monochromator's reflecting planes, in the direction of increasing k_1, and of magnitude $\alpha_1 k_1 \csc\theta_1$, where α_1 is the angular width of the entrance collimator and θ_1 the Bragg angle at the monochromator). The vector $(\Delta_c\mathbf{k}_1,\ \mathbf{k}_1\cdot\Delta_c\mathbf{k}_1)$ describes both the direction and the width of the distribution about $(\mathbf{K},\epsilon)$ in this case. If it is parallel to the dispersion surface, the opening-up of the entrance collimator has not adversely affected the energy resolution: the condition for this focusing is $(\mathbf{k}_1-\mathbf{m})\cdot\Delta_c\mathbf{k}_1=0$, where $\mathbf{m}$ is the slope of the dispersion surface, i.e., $\mathrm{grad}\mathbf{Q}\omega(\mathbf{Q})$. If the exit collimator is now opened up, the distribution about $(\mathbf{K},\epsilon)$ becomes a flat disk, the convolute of the distributions defined by $(\Delta_c\mathbf{k}_1,\ \mathbf{k}_1\cdot\Delta_c\mathbf{k}_1)$ and $(\Delta_c\mathbf{k}_2,\ \mathbf{k}_2\cdot\Delta_c\mathbf{k}_2)$. If the focusing conditions $(\mathbf{k}_1-\mathbf{m})\cdot\Delta_c\mathbf{k}_1=0$ and $(\mathbf{k}_2-\mathbf{m})\cdot\Delta_c\mathbf{k}_2=0$ are both satisfied, the disk is parallel to the dispersion surface, and the energy resolution is still unchanged. When the mosaic width of the monochromator is taken into account, the distribution of incident momenta about $\mathbf{k}_1$ is the convolute of one with width $\Delta_c\mathbf{k}_1$ and another with width $\Delta_w\mathbf{k}_1$ (a vector in the direction of $\mathbf{k}_1$, of magnitude $\beta_1 k_1 \cot\theta_1$, where β_1 is the mosaic width of the monochromator crystal). This distribution has pronounced elongation roughly in the direction of $\Delta_c\mathbf{k}_1(\Delta_w k/\Delta_c k$ is typically 0.2–0.4, and the angle be-

tween the vectors $\Delta_w\mathbf{k}$ and $\Delta_c\mathbf{k}$ 25°–50°). Consequently, when the mosaic widths of monochromator and analyzer are taken into account, the intensity distribution around $(\mathbf{K},\epsilon)$ still has its major dimensions similar to the plane disk described above, and the focusing conditions give energy resolution near the optimum.

In arranging an experiment to satisfy focusing requirements the first step is to choose $\mathbf{Q}$ (given $\mathbf{q}$ and a typical direction for $\mathbf{q}$) in a favorable direction for the phonon's polarization vector (nothing to do with focusing) and for $\mathbf{m}$. Then with $\mathbf{Q}$ known and ω guessed, the vector triangle $\mathbf{Q}=\mathbf{k}_1-\mathbf{k}_2$ is determined ($k_1^2-k_2^2=2\omega$), apart from the component of $\mathbf{k}_1$ and $\mathbf{k}_2$ perpendicular to $\mathbf{Q}$. Diagrams or tables or a computer program then show how to choose this component for a given monochromator crystal so that the focusing condition, "$(\mathbf{k}_1-\mathbf{m})$ parallel to the monochromator normal," is fulfilled, whereupon the analyzer crystal can be chosen to fulfill the focusing condition at the analyzer. An important factor here is the beam path: whether or not the sense of scattering at the sample is the same as that at the monochromator (or at the analyzer), there being four alternatives. The spectrometer setting thus arrived at applies to the peak of the expected resonance, of course, and the spectrometer is then programmed to traverse this position and record the actual resonance.

In practice, focusing is seldom exact, but even approximate focusing is valuable. Two advantages have already been pointed out—with focusing, the peak intensity is higher and the resolution width narrower (compare the use of the "parallel" position in diffractometry). Another advantage is that a source of error in the assignment of a point on a dispersion curve is removed: when focusing is exact, the true mean values of the directions of $\mathbf{k}_1$ and $\mathbf{k}_2$ need not be known exactly, because any errors merely shift the assigned point along the dispersion surface.

4. RESOLUTION. PHONON WIDTHS

To calculate the energy resolution, energies are projected on to a common ordinate along planes parallel to the dispersion surface at the point concerned. Four independent contributions to the resolution width are treated separately, then combined by adding squares and taking the root of the sum. The latter procedure is strictly appropriate when applied to the standard deviations of linear distributions that are folded together, but we can apply it to widths at half-maximum because these bear a very nearly constant ratio to the standard deviations of the distributions we are concerned with (the ratio is 2.36 for a Gaussian distribution, 2.45 for a triangular, so a figure of 2.4 is accurate within 2% for our distributions, which lie between the Gaussian form and a blunted triangle). The basic formula for each contribution to the energy resolution is $\Delta\epsilon'=(\mathbf{k}-\mathbf{m})\cdot\Delta\mathbf{k}$ (ϵ' is energy relative to the tangent to the dispersion surface, which has slope $\mathbf{m}$; $\mathbf{k}$ is the average wave vector for neutrons (either incident or scattered); $\Delta\mathbf{k}$ is $\Delta_c\mathbf{k}_1$, $\Delta_w\mathbf{k}_1$, $\Delta_c\mathbf{k}_2$, $\Delta_w\mathbf{k}_2$, respectively (see Sec. 3). The calculated resolution widths are accurate within 10%, which is quite adequate, since counting statistics make the widths of observed resonances considerably more uncertain. Where the dispersion surface has marked curvature, e.g., near the $\mathbf{q}$ origin, a correction may be made, but in the present measurements this has always been insignificant.

To extract a phonon width (still the width at half-maximum) from an observed resonance width, we have used the same simple rule for combination of squares of widths mentioned above. This procedure is open to the objection that the assumption of a 2.4 ratio between the width and the standard deviation is not even approximately valid if the line shape for the phonon is of Lorentz type. However, when we estimate the width of an observed resonance, the first step is to subtract background, and in doing so the wings of the resonance are cut off within about 1.5 times the width from the center of the resonance. If the resolution width is obviously smaller than the observed width, the phonon width extracted by the above rule corresponds to a frequency distribution cut off at the base so that the wings do not extend more than Γ or 1.5Γ from the center (Γ is the phonon width). If the line shape were Lorentzian, our rule applied to the curtailed distribution should give Γ within 15%. It will be seen from Figs. 2(a), (b), and (c) that the margins of error for phonon widths are usually much larger. If the resolution width is comparable to the observed width, and if the true line shape is such that the wings make a much larger contribution to the second moment than our rule for extracting the line width takes into account, the phonon widths arrived at will tend to be too large. But on the whole lines have been well resolved, and where resolution is poorer the margins of error for the assigned width are larger. We may thus conclude that our phonon widths are fair approximations, whatever the line shape for the phonon.

A necessary reservation here is that a phonon width derived as above may be affected by unresolved unevenness of the dispersion surface (e.g., a Kohn anomaly).

Nowhere did we observe asymmetry of a resonance which was definitely outside the probable limits associated with counting statistics.

5. DISTURBANCES

There are other processes than one-phonon scattering which may lead to peaks in the detector counting rate. If the disturbance is obvious it may be tolerable, but if small and unexpected it may lead to displacement and distortion of an observed one-phonon peak. We have observed several cases of disturbances, and have arrived at ways of eliminating them. A complete account would be out of place here, but a very brief one

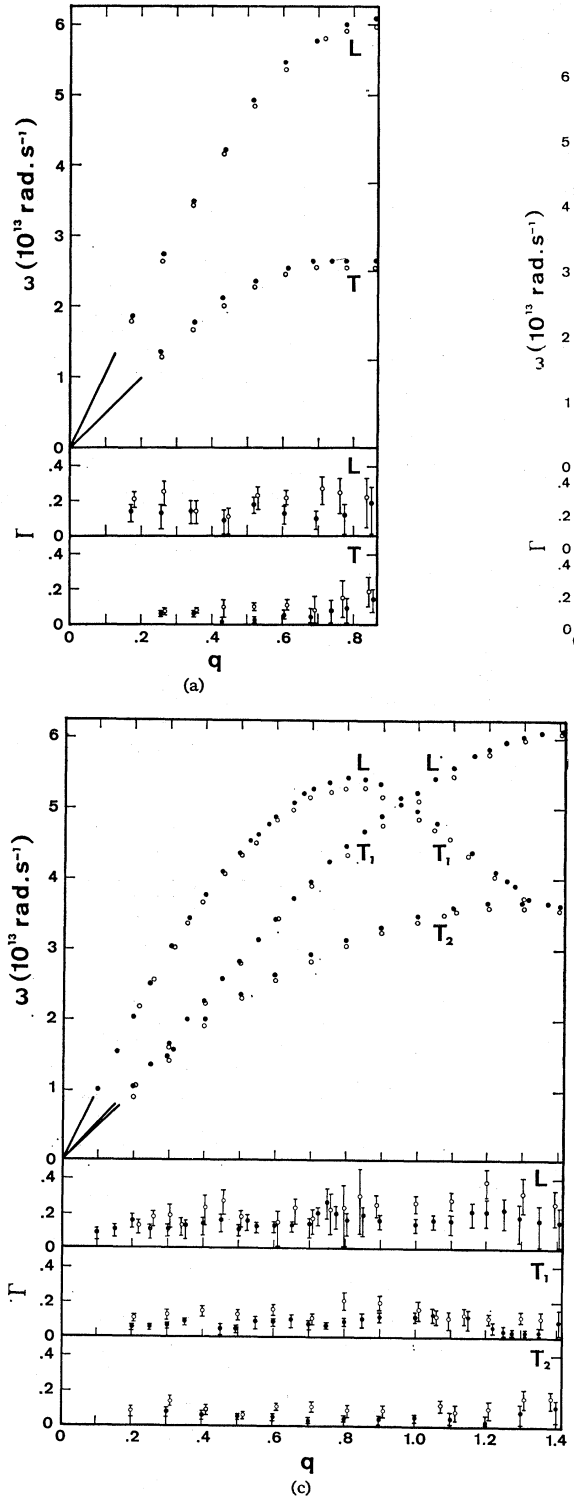

FIG. 2. Dispersion curves for aluminium at 80°K (•) and 300°K (○): (a), [1,1,1] direction; (b), [2,0,0] direction; (c) [2,2,0] direction. Underneath are corresponding phonon widths (the same frequency unit).

does at least indicate that we have been aware of the effects and have taken steps to avoid them.

The neutrons concerned here must have undergone scattering in monochromator, sample, and analyzer crystals before entering the detector. We may safely assume that the resulting intensity is negligible unless the scattering in at least two crystals is Bragg scattering, while in the remaining crystal it may be Bragg scatter-

ing, incoherent elastic scattering, coherent inelastic scattering, or in cases where there is a flat optical branch of the dispersion surface, incoherent inelastic scattering. Bragg scattering in the monochromator and analyser crystals may be in the first order or higher orders—for us the only case of significance is the second order at the analyzer. Bragg scattering in the sample may be from any set of planes, or from polycrystalline material in or near the sample, or from some small monocrystalline inclusion in the sample. These comments suffice to indicate that there are several combinations that may give rise to peaks. The most important is that where the monochromator functions normally, but the analyzer reflects in second order, and a peak is observed which arises from one-phonon scattering in the sample.

Two other effects associated with Bragg scattering in the sample are attenuation of the incident or scattered beam, giving rise to distortion of the observed peak, and a shift in the $\mathbf{Q}$ vector ($\mathbf{k}_1$ or $\mathbf{k}_2$ may be shifted by a lattice vector, giving the same shift in $\mathbf{Q}$). Brockhouse has reported that the latter effect may lead to the observation of transverse peaks in situations where they are not expected to occur because the nominal $\mathbf{Q}$ is perpendicular to the phonon's polarization. It is also conceivable that an observed peak may be distorted by superposition of resonances from the same $\mathbf{q}$ but different $\mathbf{Q}$'s (resolution and distortion may differ in the two cases). These effects were of no importance in our measurements, because the sample transmitted at least 90% of the incident neutrons even when oriented for Bragg reflection.

The following remedies are of general value.

1. Improved resolution reduces the region of $(\mathbf{K},\epsilon)$ space required for a measurement, and thus reduces the possibility of disturbances.

2. Sample crystals of more nearly perfect structure reduce the intensity and likelihood of Bragg scattering in the sample.

3. Diagrams or computer programs may be used to avoid awkward scattering situations, involving, for example, second-order reflection at the analyzer or Bragg reflection at the sample.

4. An analyzer with no second-order reflection—e.g., Ge(1,1,1)—prevents what is perhaps the most important disturbance (we are not yet able to apply this remedy).

5. The sample may be tilted a few degrees about $\mathbf{K}$, so that the scattering plane is no longer a plane of high symmetry, containing many reciprocal lattice points. This diminishes the likelihood of Bragg scattering from the sample into the analyzer, and of one-phonon scattering associated with low-energy phonons and second-order reflection in the analyzer.

6. A monitor in the beam entering the analyzer discloses Bragg scattering from the sample towards the analyzer, as well as attenuation of the incident or scattered beams due to Bragg scattering in the sample.

6. RESULTS AND ERRORS

6.1. Results

Dispersion curves for the [1,1,1], [2,0,0], and [2,2,0] directions are shown in Figs. 2(a), (b), and (c). They are for 80 and 300°K. Below them are the corresponding phonon widths, determined as described in Sec. 4. The units for Γ and ω are the same. Wave numbers are expressed in natural units for aluminum ($2\pi/$(the side of the unit cube), i.e., 1.561 Å^{-1} at 80°K, 1.555 Å^{-1} at 300°K). It should be noted that the labelling of the [2,2,0] L and T_1 branches is in accordance with the continuous dispersion surfaces illustrated in Figs. 3(a), 3(b), and 3(c), which involves a discontinuity in the polarization at the intersection of the curves. The lines through the origin in each case have slopes corresponding to the appropriate velocity of sound in the direction concerned, from measurements at 80°K and 10 MHz.[6]

Figures 3(a), 3(b), and 3(c) are derived from the dispersion curves, together with further measurements at the sites marked "+." They show energy contours on the inner surface of an elemental tetrahedron in reciprocal space—indicated by the small insets accompanying each figure. The tetrahedron corresponds to a segment of the first Brillouin zone which is 1/48 of the while, except that the boundary opposite the origin is simplified.

6.2. Errors

In assigning a mean position to a resonance, an estimate is made of the limits within which this position probably lies, taking into account the shape of the resonance and the counting statistics. ("Probably" here is not well defined, of course; we may say that it roughly corresponds to 0.7 probability). The estimated error is typically 0.02×10^{13} rad sec^{-1}. (Repetition of the unit 10^{13} rad sec^{-1} after each frequency value is tedious, so we will let the unit be understood from now on.) In some places it is lower, e.g., for much of the transverse branches, where most of the observed resonances were narrow, and in others higher—e.g., 2 to 3 times larger near the highest frequencies of longitudinal branches, where resonances were broad and intensities low.

Errors associated with angular calibrations or collimator widths are considered to be negligible by comparison with the above error, except perhaps on the steepest part of transverse branches (where, for instance, an error of about 0.03° in the orientation of the sample would lead to an error of about 0.001 in q and about 0.01 in ω). Several of the points shown in the figures are averages of two or more measurements, and such measurements have always been consistent.

An error may arise from the curvature of a dispersion surface, since the spectrometer records an average for an appreciable region of $\mathbf{K}$ space. However, resolution in $\mathbf{K}$ space was typically about 0.07 in all direc-

[6] G. N. Kamm and G. A. Alers, J. Appl. Phys. 35, 327 (1964).

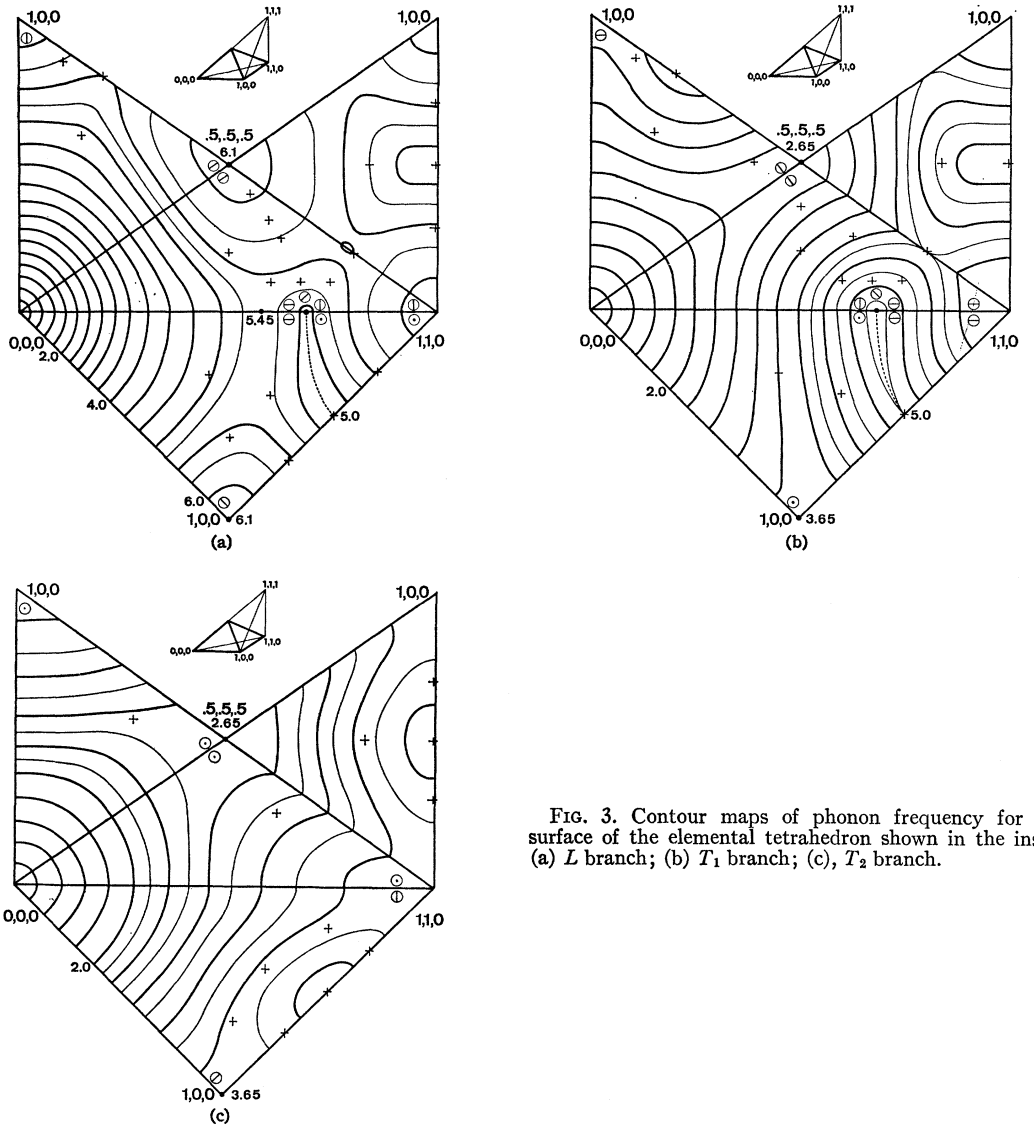

FIG. 3. Contour maps of phonon frequency for the inner surface of the elemental tetrahedron shown in the inset. 80°K. (a) L branch; (b) T_1 branch; (c), T_2 branch.

tions (the same units as q in the figures), and it can be shown that the error due to curvature of the surface is then negligible, with occasional exceptions at small q, where a small correction has been made.

Errors have not been indicated for points on dispersion curves, but the size of the points corresponds to an error of 0.03. Errors for widths of resonance as observed have been estimated by inspection of resonance plots with counting statistics inserted. The error for the computed resonance width has been regarded as negligible by comparison, so the errors for the phonon width Γ given in Figs. 2(a), (b), and (c) are derived entirely from the estimated errors for observed resonances. A characteristic effect of the procedure used to extract Γ from observed widths is that the error in Γ tends to be larger in the negative direction than in the positive.

A spurious broadening of phonons associated with mosaic structure in the sample is worth noting. When mosaic is taken into account, the reciprocal space of the crystal becomes slightly blurred: the uncertainty for a wave vector $\mathbf{Q}$ is βQ perpendicular to $\mathbf{Q}$, if β is the mosaic width. If the dispersion surface under examination has slope m_y perpendicular to $\mathbf{Q}$, there will be a contribution $\beta m_y Q$ to observed phonon widths. For most longitudinal phonons this contribution is zero, because $\mathbf{Q}$ is usually in a symmetry direction, but for transverse branches it may be appreciable. For our sample a typical value of this width contribution for transverse phonons would be 0.02, which is almost negligible, but the crystal was unusually good, and for many commercial crystals an effect some 4 times as large might be expected.

7. COMMENTS

7.1. Dispersion Curves

The curves have no particularly obvious irregularities, but if an average value of the slope is calculated for the interval between consecutive points, and this slope plotted against q, irregularities are revealed which are significant in relation to the errors involved. Such analysis has indicated nine Kohn anomalies. Two of them, at $q=0.83$ on the [2,0,0] L curve and $q=0.72$ on the [1,1,1] T curve, are discernible in the figures shown here. However, this matter has been treated separately elsewhere.[1]

Another interesting feature of the slope-versus-q plots is the behavior near the origin. If the slope at the origin is taken from the velocity of sound at 10 MHz,[6,7] our first value of the slope is nowhere lower than this. A significant initial rise in slope occurs for all the transverse branches, and this negative dispersion is particularly marked for the [2,2,0] T_1 and T_2 branches.

Yarnell and Warren[8] have made detailed measurements on phonons in the [2,0,0] and [2,2,0] directions of aluminum at 300°K. Our corresponding curves agree with theirs well within stated margins of error, except around the maximum of the [2,2,0] L curve near $q=0.8$, and near the maximum of the [2,0,0] T curve. In both cases their ω values are about 0,1 larger than ours. In the first case the scatter of their points is rather large— measurements are difficult in the region concerned. In the second case their results are not consistent with the [2,2,0] T_1 and T_2 frequencies at $q=1.414$, which by symmetry are the same as the [2,0,0]T frequency at $q=1.0$. The discrepancy could be explained by a slight error in the adjustment of their sample: it will be seen from our Fig. 3(b) that the T_1 frequencies in the [2,0,0] direction near [1,0,0] lie in a notably narrow valley, which means that even quite a small error in the "vertical" adjustment entails an upward shift of frequencies in this neighborhood.

Vosko *et al.*[9] have recently attempted to fit theoretical dispersion curves to experimental data for aluminum (they give references to earlier, less comprehensive work). Fair agreement is obtained for longitudinal branches, but, as they point out, the results for transverse branches leave something to be desired. It seems that the discrepancies are connected with the difficulty in deciding the short-range behaviour of the ion-electron potential (see Ref. 9, pp. 1205, 1206), evidently a formidable theoretical problem.

[7] On the basis of anharmonic theory the slope at the origin should correspond to the isothermal elastic constants [H. Hahn, *Inelastic Scattering of Neutrons in Solids and Liquids I*, (International Atomic Energy Agency, Vienna 1963), p. 48], not to the adiabatic constants of Ref. 5, but in aluminum the isothermal values are only about 0.5% lower for the longitudinal branches at both temperatures, and the same as the adiabatic for the transverse branches.

[8] *Lattice Dynamics* edited by R. F. Wallis (Pergamon Press, Inc., New York, 1965), pp. 57–61.

[9] S. H. Vosko, R. Taylor, and G. H. Keech, Can. J. Phys. **43**, 1187 (1965).

The frequency maps of Figs. 3(a) 3(b), and 3(c) demonstrate that relatively few measurements in off-symmetry directions suffice for reliable interpolation of phonon frequencies, merely utilizing boundary symmetries and without assumptions about interatomic forces. Actually, this interpolation has been carried a step further, to give frequency tables for the three branches over a cubic network (q interval 0.1) covering the whole first zone. Copies of the tables may be obtained on request.

7.2. Shifts of frequency from 80 to 300°K

In two-thirds of the cases where measurements were made on phonons with the same q at both 80 and 300°K the downward shift in frequency when the temperature increased was between 0.05 and 0.10 (the over-all average shift was 0.075). Because of the general uniformity of the shift, for all directions and both longitudinal and transverse branches, together with the fact that the shifts are subject to the errors for the individual frequencies (see Sec. 6.2), no distinct trends can be observed. We could have followed shifts more accurately by making measurements at different temperatures soon after one another, but for experimental convenience we seldom did so. Shifts on the [2,0,0]L, [2,2,0]L, and [2,2,0]T_1 branches around $\omega=5.2$ are large (up to 0.18). In Sec. 7.3 a suggestion is put forward that an anomalous broadening of phonons in the same region may be associated with a singularity in the phonon-phonon interaction there, and such a singularity might also lead to an anomalously large shift[10]; however, errors in the region concerned are large, and the observation may not be significant.

Temperature shifts in aluminum have previously been studied by Larsson *et al.*[11] from 300°K up to the melting point. They find a uniform shift of 0.1 per 100°C for four phonons with frequencies between 3 and 5. The shift per unit temperature difference falls to zero towards 0°K, so our considerably smaller shift is as expected. Hahn[7] has compared the measured shifts of Larsson *et al.* with a theoretical curve, and found good agreement. The curve is also in fair agreement with our results, if we compare twice our average relative shift in the slopes of longitudinal curves (ω versus q) for small q (our result is 0.06 ± 0.01) with the shift in Hahn's function (which involves relative values of ω^2 for small q; the shift in his function between 80 and 300°K is 0.09). The corresponding quantity for the ultrasound data is 0.06.

7.3. Frequency Widths of Phonons

The margins of error in the determination of phonon frequency widths are inevitably rather large, but

[10] See R. A. Cowley, in *Lattice Dynamics* edited by R. F. Wallis, Pergamon Press, Inc., New York, 1965), pp. 295–303. In particular, see the general formulas for shifts and widths on p. 296.

[11] K-E. Larsson, U. Dahlborg, and S. Holmryd, Arkiv Fysik **17**, 369 (1960).

nevertheless some general features and trends in the widths of Figs. 2(a), 2(b), and 2(c) are apparent on inspection. Transverse phonons at 80°K are usually narrower than longitudinal phonons, but this difference tends to disappear at 300°K. In two places—near the maxima of the $[2,0,0]L$ and $[2,2,0]L$ branches at 300°K—widths are exceptionally large. Plausible explanations of these observations may be obtained by supposing that widths are mainly governed by the phonon-electron interaction at 80°K (a low temperature compared to the Debye temperature, 390°K), while phonon-phonon processes dominate at 300°K.[12] The main features of the phonon widths at 80°K may be interpreted with the aid of a formula given by Woll and Kohn[12] for widths due to the decay of phonons into electron-hole pairs. The anomalous broadening at the two places mentioned may be attributed to a singularity in the phonon-phonon interaction, which would also account for the relatively large phonon widths in the regions concerned even at 80°K.

The formula given by Woll and Kohn is of the form

$$\Gamma_e=\sum_{\mathbf{G}}(\mathbf{Q}\cdot\mathbf{e}/Q)^2A(Q)\,, \qquad (1)$$

where Γ_e is the phonon width due to phonon-electron interaction, and $\mathbf{e}$ is the polarization vector of the phonon. $A(Q)$ rises from the origin to a maximum value somewhere in the region $Q<1$, and then falls off to a relatively small value at $Q=2$; at $Q=2k_F$ (k_F is the Fermi radius, 1.13 for aluminum) it falls abruptly to zero, and this drop corresponds to Kohn anomalies in Γ_e. The more exact behavior of $A(Q)$ for large Q is important for any calculation of widths, but it is subject to the same theoretical diffculty regarding the short-range part of the ion-electron potential that was mentioned in another connection in Sec. 7.1. Woll and Kohn have calculated phonon widths for the (1,1,1) L and T branches in aluminum, using an approximation for $A(Q)$ which as they point out falls off too slowly, in order to demonstrate the anomalies just mentioned (difficult to observe experimentally, and not observed by us). This illustrative calculation leads to a result that is clearly at variance with experiment: the calculated longitudinal and transverse widths are of about the same size, which is too large in the transverse case. It is an easy matter to write down sums (1) for any $\mathbf{q}$ and $\mathbf{e}$, since the number of $\mathbf{G}$'s is less than 20, because of the restriction to $Q<2.26$, and moreover these fall into symmetry groups. Approximating by shifting all Q values to the nearest one in the sequence 0.1, 0.2, $\cdots$, 2.2, it is found that for each $\mathbf{q}$ and each polarization, Γ_e is the sum of from 3 to 6 terms of the form: (known number)$\times A$ (known Q). Because $(\mathbf{Q}\cdot\mathbf{e}/Q)^2$ is zero for transverse branches when $\mathbf{G}=(0,0,0)$ or when $\mathbf{G}$ is some other relatively close point (e.g., $\mathbf{G}=(1,1,1)$ for the (1,1,1) branches) the transverse sums have no terms for $Q<1.3$, while the longitudinal sums have terms roughly similar to the transverse for $Q>1.3$, together with terms for $Q<1.3$ (the $\mathbf{G}=(0,0,0)$ term is especially important). Interpretation of the observed widths evidently requires that the terms for $Q<1.3$ dominate markedly in the longitudinal sums. In Woll and Kohn's calculation this requirement is not met, and the calculated longitudinal and transverse widths are therefore similar. It is possible to go further in the interpretation of our width data, and to derive some naturally very approximate values of $A(Q)$ by comparing the sums mentioned above with the experimental widths. For instance, experimental widths for all longitudinal phonons in the region $0.3<q<0.7$ are quite similar, and the corresponding similarity of the sums (1), in which the $\mathbf{G}=(0,0,0)$ term dominates, allows values to be assigned to $A(Q)$ in this region: we take $A(0.6)\approx 0.10$, and the maximum of $A(Q)$ to be at $Q=0.6\pm 0.1$. The measurements near $q=1.3$ on the $[2,2,0]T_1$ branch are particularly accurate, and unaffected by the slight apparent broadening of transverse phonons due to mosaic structure (see Sec. 6.2) because the measurements were made with $\mathbf{K}$(or $\mathbf{Q}$) parallel to $\mathbf{e}$; they yield $A(1.3)\approx 0.02$. The transverse sums are almost everywhere dominated by a term which is typically $1.7A(1.6)$; the experimental values are also generally similar, so $A(1.6)\approx 0.01$ (taking into account the broadening effect just mentioned). (For $[2,2,0]T_1$ phonons and $q<0.96$ there are terms for $Q<1.6$, arising from $\mathbf{G}$'s such as (1,1,1), and the experimental widths are correspondingly higher than for other transverse branches.). Values of $A(Q)$ calculated from Woll and Kohn's Eq. 4.4 with $m^*=m$, $W^*(p)=W(p)$ and $v^*(p)=4\pi G(pr_s)/p^2$ are: $A(0.6)=0.06$, $A(1.3)=0.007$, $A(1.6)=0.0006$. This $A(Q)$ falls off too rapidly, which was only to be expected from the simple form adopted for $v^*(p)$ (See Ref. 9, p. 1232 and elsewhere, and Ref. 13, Eq. 3.8). No attempt has been made to obtain a fit by adjusting $v^*(p)$, because that would be pressing our very approximate results too far; we merely wish to point out that an interpretation of phonon widths along the above lines is quite feasible.

Three regions in which the interpretation of phonon widths at 80°K in terms of the phonon-electron interaction as outlined above leads to values which are too low are: the $[2,0,0]L$ branch around $q=0.8$, and the $[2,2,0]$ branch around $q=0.8$ and $q=1.2$. The frequencies in the three cases are around 5.2. In the first and third cases the widths at 300°K are also unusually large, as repeated measurements have confirmed, while in the second case the situation is not clear because the measurements at 300°K were of poorer quality. If we confine ourselves to the first and third cases, the observed effects may be attributed to a singularity—not sharply defined, of course—in the phonon-phonon interaction, with the phonons concerned decaying into

[12] See R. J. Elliot and H. Stern, *Inelastic Scattering of Neutrons in Solids and Liquids* (International Atomic Energy Agency, Vienna, 1961), p. 68, Discussion.

[13] E. J. Woll and W. Kohn, Phys. Rev. **126**, 1693 (1962).

two phonons having wave vectors in the neighborhood of points like (0.4,0.4,0.4) and frequencies near 2.6. The conditions $\omega=\omega_1+\omega_2$ and $\mathbf{Q}=\mathbf{Q}_1+\mathbf{Q}_2$ can be fulfilled simultaneously in this neighborhood (ω, $\mathbf{Q}$ refer to the primary phonon, ω_1, $\mathbf{Q}_1$, ω_2, $\mathbf{Q}_2$ to the secondary phonons) if we take $\mathbf{Q}_1$ near (0.4,0.4,0.4) and $\mathbf{Q}_2$ near (0.4, −0.4, −0.4) for case 1 and $\mathbf{Q}_1$ near (0.4, 0.4, 0.4), $\mathbf{Q}_2$ near (−0.4, 0.4, 0.4) for case 3. The secondary phonons here are near the flat maximum of the $[1,1,1]T$ curve, and we may expect a high density of states on the final side of the transition. Unfortunately, proper confirmation of this suggested singularity calls for a major effort of computation which is beyond our scope; the argument put forward here is merely one of plausibility.

ACKNOWLEDGMENTS

We have of course received help from many sources in building and running the spectrometer. It is a particular pleasure to acknowledge the technical assistance given by K.-O. Isaxon at all stages. Dr. R. Pauli has given us the support of close interest throughout.

PHYSICAL REVIEW VOLUME 145, NUMBER 2 13 MAY 1966

Second-Order Optical Processes and Harmonic Fields in Solids

SUDHANSHU S. JHA
Tata Institute of Fundamental Research, Bombay, India
(Received 13 December 1965)

A consistent method has been developed to calculate induced electromagnetic fields and optical transitions of electrons in a solid, in response to an incident laser beam of (circular) frequency ω. The analysis is based upon the independent-particle Schrödinger equation for electrons and Maxwell's equations for the electromagnetic fields. General expressions for linear and bilinear currents as well as second-order optical transition probabilities have been derived. It is shown that the second-order transition probability, which is proportional to the fourth power in the incident field, contains two different types of terms, describing double-photon transitions of the incident frequency ω and single-photon transitions of the harmonic frequency 2ω. An estimate has been made to show that in the case of centrosymmetric solids like metals, the relative contribution due to the single second-harmonic photon transition is of the order $(e^2/\hbar c)^2 \ll 1$ in the optical region, compared with the double-fundamental-photon transition. However, in the case of solids lacking inversion symmetry, the contributions due to these two processes are estimated to be of the same order in magnitude.

1. INTRODUCTION

AFTER the discovery[1] of lasers it has now become possible to observe[2] second-order optical transitions of electrons in solids. Usually one assumes[3] the physical process involved in such cases to be either emission or absorption of two photons of incident (circular) frequency ω. However, the powerful laser beams required for these observations also produce harmonic fields in the solid. An electron in the solid does not move in the incident field of frequency ω but in a self-consistent local field which contains the fundamental field proportional to the incident field, and other harmonic fields of higher order in the incident field. In particular, the second harmonic field is proportional to the square of the incident field. Contributions to the second-order optical transition probability proportional to the fourth power of the incident field may therefore come not only from double-photon transitions of the fundamental field but also from single-photon transitions of the induced second harmonic field. The purpose of this paper is to study the relative importance of these two processes.

Several theoretical calculations[4–9] of nonlinear polarizability, from which induced fields may be deduced by solving[10] Maxwell's equations, have been published. These methods are distinguished by the nature of simplifying assumptions and by the stage at which they are introduced. However, in most of these investigations only electric-dipole transitions have been considered and they have therefore only restricted applications.

[1] A. L. Schawlow and C. H. Townes, Phys. Rev. **112**, 1940 (1958).
[2] W. Kaiser and C. G. B. Garrett, Phys. Rev. Letters **7**, 229 (1961); I. D. Abella, *ibid.* **9**, 453 (1962); J. F. Porter, *ibid.* **7**, 414 (1961); D. H. McMahon and K. M. Kestigian, Phys. Rev. (to be published); A. Gold and J. P. Hernandez, *ibid.* **139**, A2002 (1965). See also other references in the last paper.
[3] D. A. Kleinman, Phys. Rev. **125**, 87 (1962); R. Braunstein, *ibid.* **125**, 475 (1962); M. Goeppert-Meyer, Ann. Physik **9**, 273 (1931); A. M. Bonch-Bruevich and Y. A. Khodovoi, Usp. Fiz. Nauk **85**, 3 (1965) [English transl.: Soviet Phys.—Usp. **8**, 1 (1965).
[4] J. A. Armstrong, N. Bloembergen, J. Ducing, and P. S. Pershan, Phys. Rev. **127**, 1918 (1962).
[5] P. L. Kelley, J. Phys. Chem. Solids **24**, 607 (1963).
[6] R. Loudon, Proc. Phys. Soc. (London) **80**, 952 (1962).
[7] P. A. Franken and J. F. Ward, Rev. Mod. Phys. **35**, 23 (1963); see also J. F. Ward, *ibid.* **37**, 1 (1965).
[8] E. Adler, Phys. Rev. **134**, A728 (1964).
[9] A. S. Pine, Phys. Rev. **139**, A901 (1965). See also other references in this paper.
[10] N. Bloembergen and P. S. Pershan, Phys. Rev. **128**, 193 (1962).